Journal of the European Ceramic Society **11** (1993) 353–358

Electrical Conductivity of AlN Ceramics at High Temperatures

W. A. Groen, J. G. van Lierop & J. M. Toonen
Philips Research Laboratories, P.O. Box 80000, 5600 JA Eindhoven, The Netherlands

(Received 22 April 1992; revised version received 22 July 1992; accepted 30 September 1992)

Abstract

The electrical conductivity of AlN ceramics with 4% Y_2O_3 and 1% CaO sintering aids has been investigated with complex impedance spectroscopy at temperatures between 600°C and 1100°C. The impedance spectrum consists of a single arc with a relatively high capacitance. This behaviour can be interpreted using the brick layer model which leads to the conclusion that the AlN grains are covered with a continuous layer of deviating composition. This is in agreement with SEM observations. The results indicate that at high temperatures the resistivity of the sample is dominated by the grain boundaries present in the ceramic AlN sample. Using the brick layer model the average thickness of the grain boundary layers is estimated to be between 46 nm and 67 nm. The results also explain the independence of the electrical conductivity at high temperatures from the nitrogen partial pressure. The activation energy for electrical conductivity was found to be 2·4 eV. From these results it is concluded that the electrical conduction is not related to the intrinsic properties of aluminium nitride.

Die elektrische Leitfähigkeit von AlN–Keramiken mit 4% Y_2O_3- und 1% CaO-Zusatz als Sinterhilfe wurden für den Temperaturbereich von 600°C bis 1100°C mittels komplexer Impedanzspektroskopie untersucht. Das Impedanzspektrum besteht aus einem einzelnen Bogen mit verhältnismäßig hoher Kapazitanz. Dieses Verhalten kann mit Hilfe des 'Brick-Layer'-Modells erklärt werden. Demnach sind die AlN-Körner von einer kontinuierlichen Schicht mit variierender Zusammensetzung umhüllt. Dieses Ergebnis ist auch in Übereinstimmung mit REM-Beobachtungen. Der Widerstand scheint bei hohen Temperaturen hauptsächlich durch die Korngrenzen in den keramischen AlN-Proben bestimmt zu sein. Mit Hilfe des 'Brick-Layer'-Modells konnte die mittlere Dicke der Korngrenzenschichten zu 46 nm–67 nm bestimmt werden. Die Ergebnisse erklären auch, warum die elektrische Leitfähigkeit bei hohen Temperaturen nicht vom N-Partialdruck abhängt. Die Aktivierungsenergie für elektrische Leitung wurde zu 2·4 eV bestimmt. Aus diesen Ergebnissen kann gefolgert werden, daß die elektrische Leitung nicht durch die intrinsischen Eigenschaften des Aluminiumnitrids bestimmt wird.

La conductivité électrique de céramiques en AlN avec 4% Y_2O_3 et 1% CaO, en tant qu'aides au frittage, a été étudiée à l'aide de la spectroscopie d'impédances complexes à des températures comprises entre 600°C et 1100°C. Le spectre d'impédance consiste en un simple arc avec une capacité relativement élevée. Ce comportement peut être interprêté avec le modèle 'brick-layer' qui conduit à la conclusion que les grains d'AlN sont couverts d'une couche continue de composition variable. Ce fait est en accord avec les observations pratiques au MEB. Les résultats indiquent qu'à haute température, la résistivité de l'échantillon est dominée par les joints de grains présents dans l'échantillon d'AlN. A partir du modèle 'brick layer', l'épaisseur moyenne des joints de grains est estimée entre 46 et 67 mm. Les résultats expliquent également la non dépendance à haute température de la conductivité électrique vis-à-vis de la pression partielle en azote. L'énergie d'activation pour la conductivité électrique est de 2.4 eV. A partir de ces résultats, les auteurs concluent que la conductivité électrique ne dépend pas des propriétés intrinsèques du nitrure d'aluminium.

1 Introduction

Aluminium nitride ceramics are currently of interest because they combine a high thermal conductivity with a high electrical resistance at room temperature. A prerequisite to evaluate the applications above room temperature is more information about the electrical properties of AlN ceramics. Regarding

Journal of the European Ceramic Society 0955-2219/93/$6.00

the electrical conductivity of AlN ceramics only a few papers have been published in which some different models are proposed to explain the high-temperature electrical conductivity.[1-3] In general, a large variety of activation energies for electrical conductivity and an independency on the partial nitrogen pressure are reported.

Francis & Worrell[1] investigated the AC and DC electrical conductivity of hot-pressed unintentionally doped polycrystalline AlN samples. The sample density was 99·8% of the theoretical density and no grain sizes are reported. The electrical conductivity was found to be independent of the nitrogen partial pressure and exhibits an activation energy of 1·82 eV. Furthermore, it was concluded that the conduction process is extrinsic, due to carbon impurities present in the AlN. Richards *et al.*[2] also reported that the conductivity is independent of the nitrogen partial pressure for hot-pressed aluminium nitride samples doped with oxygen and beryllium. Grain sizes are not given. The activation energy for electrical conduction was found to be between 1·45 and 1·57 eV. Beryllium doping resulted in a decrease of the conductivity. From these results it is concluded that the charge carriers are intrinsic electrons or aluminium vacancies. Predominant ionic conduction for AlN has also been reported by Yahagi & Goto[3] who performed DC polarisation and EMF measurements. An activation energy of 1·75 eV has been determined for a sample containing 2 wt% of Y_2O_3 while for a sample containing 2 wt% of Al_2O_3 a value of 2·07 eV has been found. Again no grain sizes are given.

As far as the dielectric properties are concerned Anbreeva & Dubovick[4] have shown that AlN can be used as a high-temperature dielectric because of the high value of the dielectric constant found. In later studies[5] the dielectric behaviour of AlN ceramics, with or without additives of MgO, BeO and Y_2O_3 with a porosity varying from 9·0 to 11·5 vol.%, has been reported. It has been observed that the dielectric constant increases with the temperature. The use of the oxidic additives makes this behaviour more pronounced. The increase in dielectric constant has been attributed to space charge polarisation which occurs as a result of various types of defects in a polycrystalline material.

The nature of the predominant defect in AlN single crystals has been described by Slack *et al.*[6] It is shown that the introduction of oxygen results in the formation of aluminium vacancies causing a drastic decrease of the thermal conductivity. Recently the same result has been reported for AlN ceramics by Harris *et al.*[7]

In this paper an investigation of the electrical properties of nearly full dense AlN, containing 1 wt% CaO and 4 wt% Y_2O_3 as sintering additives, with complex impedance spectroscopy is described. Complex impedance spectroscopy makes it possible to characterise the electrical properties of many electronic materials. The technique is especially suited for polycrystalline materials, since it is possible to distinguish between the contribution of the grains and the grain boundaries to the electrical behaviour. An introduction to the method of complex impedance spectroscopy and its applications to the characterisation of materials is given in Ref. 8.

2 Experimental

The sample was prepared from AlN powder (Tokuyoma Soda, F-grade, typical particle size 1 μm). To achieve homogeneous mixing of the sintering additives these were added to a dispersion of AlN powder in ethanol as a solution of yttrium acetylacetonate in ethanol and a solution of $Ca(NO_3)_2.4H_2O$ in ethanol in the appropriate ratios. After the additions of the dopant solutions, ethanol was evaporated at about 70°C under stirring. From the resultant powder mixture pellets were pressed using a PMMA die at 5 MPa. These pellets were subsequently cold isostatically pressed at 100 MPa and thereafter calcinated at 600°C for 1 h in a dry O_2/N_2 flow (1:4). Sintering of the pellets was performed, one by one, in an Astro-W furnace in a N_2/H_2 flow (24% H_2) at a pressure of 1020 mbar. The heating rate was 10·000°C/h to the set point of 1750°C. The sample was kept for 5 h at this temperature and was cooled down to room temperature at a rate of 200°C/h. After sintering the bulk density was measured by the Archimedes method in water.

The crystalline phases present in the ceramic AlN were investigated at room temperature with X-ray diffraction using monochromatized Cu-K_α radiation. The oxygen content was measured using a Leco TC 436 O_2/N_2 analyser and the carbon content has been determined using a Strohline Coulomath 702 C/S analyser.

The electrical measurements were performed in a home-built horizontal tube furnace in which the sample is centrally placed. A schematic drawing of the geometry around the sample is given in Fig. 1. The sample is placed in a guarded sample holder to prevent surface conduction. The sample holder is situated on top of an alumina tube which is coaxially positioned inside a larger alumina tube in the furnace. The chosen geometry makes it possible to exclude gas conduction. The furnace is heated by a SiC element which is driven by a DC power supply. The maximum temperature which can be reached is 1600°C. The temperature of the sample is monitored

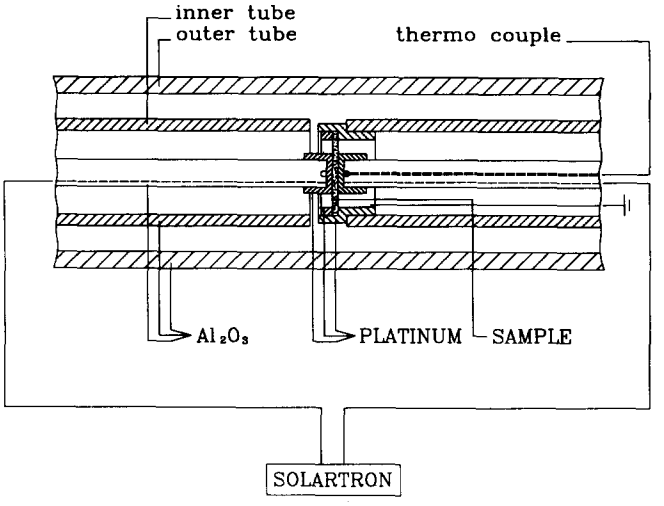

Fig. 1. A schematic drawing of the sample geometry.

using an S-type thermocouple which is positioned behind the Pt electrode (see Fig. 1). The temperature in the furnace is stable to within 0·1 °C.

The contacts on the AlN pellet (thickness: 0·045 cm, diameter 1·5 cm) were made by sputtering 0·25 μm Pt. Thereafter the contacts were painted over with Pt paste (Demetron). The paste was baked out at 600 °C for 1 h in a dry N_2/O_2 flow (4:1) and 1 h at 1200 °C in pure N_2 in an Astro-C furnace. The electrical measurements were performed in a flow of H_2/N_2 (24% H_2) and in a purified N_2 flow ($\log p_{O_2} = -6$) with a pressure of 1100 mbar. The complex impedance measurements were made using a Solartron 1250 frequency response analyser and a Solartron 1274 electrochemical interface. The data were analysed using the program EQUIVALENT CIRCUIT written by Boukamp.[9] Capacitance measurements were made in the same set-up using a Philips PM6303 LCR meter with operating frequency of 1 kHz.

3 Results

The sintered pellets are white. The resulting density of the sintered pellets is 3·31 g/cm^3 which is slightly higher than that of pure AlN (3·25 g/cm^3). This is due to the second phases present in the sample. The second phases identified with X-ray diffraction were $YAlO_3$ and $Y_3Al_5O_{12}$. No traces of any calcium-containing phases were observed. The concentration of these phases may be below the detection of X-ray diffraction. Alternatively, evaporation of calcium may occur during sintering. It is of interest to note that calcium depletion was also observed in calcium-doped AlN ceramics using neutron activation analyses. The oxygen and carbon content in the sintered specimen are 2·5(1) wt% O and about 150 ppm C, respectively.

The microstructure of the sintered sample was examined using a scanning electron microscope (SEM) to determine the grain size and the morphology of the second phases. In Fig. 2(a) and (b) SEM micrographs are shown of a fractured sample and a polished surface. The micrographs show that full density has been achieved. Furthermore, a substantial amount of second phase is visible. The second phases ($YAlO_3$ and $Y_3Al_5O_{12}$) are mainly present at triple points between the AlN grains but may also be present as a continuous layer covering the AlN grains. The median grain size for the AlN particles was estimated visually at about 6 μm by line analysis. To obtain more information about the morphology of the second phases a polished sample was etched in a saturated KOH solution in water at room temperature for 4 h. In an alkaline solution AlN slowly decomposes while the second phases like $YAlO_3$ and $Y_3Al_5O_{12}$ are insoluble. SEM micrographs of an etched sample are shown in Fig. 2(c) and (d). These micrographs clearly show the existence of a thin continuous phase covering the AlN grains.

The complex impedance measurements were all done at 0·5 V. No changes in the signals were observed on decreasing the voltage to 0·05 V. However, irreproducible effects were sometimes observed on increasing the voltage above 1·0 V. The measurements are performed from 65000 Hz down to 0·1 Hz. Those performed in purified N_2 and those which were performed in a H_2/N_2 mixture (24% H_2) gave similar results. A typical impedance plot of a measurement, performed at 750 °C, and the simulated plot are presented in Fig. 3. Generally, complex impedance plane plots of polycrystalline samples show three semicircles corresponding to bulk conductivity, grain boundary conductivity and electrode effects, respectively. For all measurements only one semicircle has been observed. Furthermore, it is observed that these circles are all depressed, which in fact means that the centre of the semicircle is placed below the real axis in the complex impedance plane. The data were fitted using an equivalent circuit of a resistance parallel to a constant phase element (CPE). No general physical interpretation has been given yet.[9] The CPE resembles the capacitance for a non-ideal dielectric behaviour. The impedance of the CPE is represented by:[9]

$$Z_{CPE} = (jw)^{-n}/Q \qquad (0 < n < 1)$$

In which Q denotes the capacitance of the CPE, n the frequency dependency of the CPE and w the frequency. Note that when $n = 1$, the CPE act as a normal capacitor.

A summary of the measurements together with the result of the corresponding non-linear least-squares fit are given in Table 1. Typical calculated

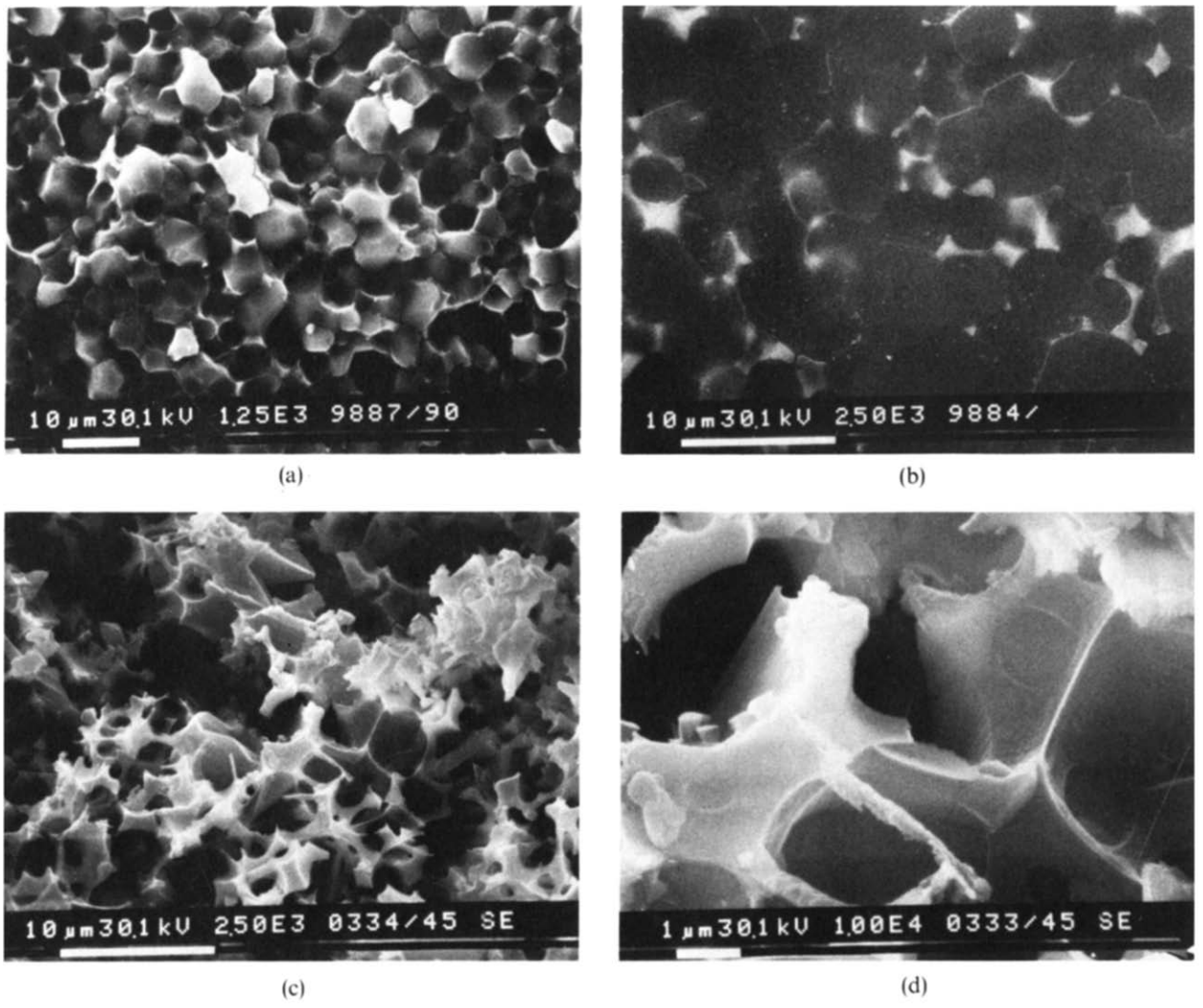

Fig. 2. SEM micrographs of (a) a fractured surface of the sintered AlN sample; (b) a polished AlN surface; (c) a polished surface which has been etched in a saturated KOH solution for 4 h; and (d) higher magnification of the micrograph in 2(c).

errors in R, Q and n are respectively $<0{\cdot}5\%$, $<5\%$ and $<0{\cdot}5\%$. Above 850°C it is impossible to simulate the plot because insufficient frequency dispersion could be observed. This is a consequence of the maximum frequency of 65 Hz of the frequency response analyser used. In this case R(calc) is taken as the intersection of the data with the X-axis.

In Fig. 4 an Arrhenius plot of the data is presented. The plot shows a difference between the data collected in the first heating cycle (up to 1000°C) and the data which were obtained during cooling.

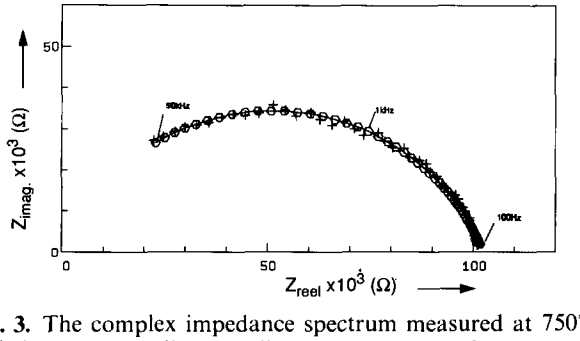

Fig. 3. The complex impedance spectrum measured at 750°C and the corresponding non-linear least-squares fit. Z_{imag} and Z_{real} denote the imaginery and real part of the impedance, respectively.

For this reason the sample was again heated to 1100°C and cooled to 800°C. The measurements made at these temperatures are shown in Fig. 4 with an extra circle. These measurements show that a reproducible resistance has been measured. The activation energy for the conduction was 2·4 eV.

The capacitance measurements were made from

Table 1. Results of the non-linear least-squares fit—indicates no calculations could be performed because no frequency dispersion could be observed. Typical calculated errors in R, Q and n are respectively $<0{\cdot}5\%$, $<5\%$ and $<0{\cdot}5\%$.

T (°C)	R(calc) (Ω)	Q(calc) (F)	n
800	$1{\cdot}4 \times 10^5$	$2{\cdot}1 \times 10^{-9}$	0·77
900	$8{\cdot}0 \times 10^3$	$1{\cdot}3 \times 10^{-9}$	0·80
1 000	$6{\cdot}3 \times 10^2$	—	—
950	$1{\cdot}4 \times 10^3$	—	—
900	$3{\cdot}3 \times 10^3$	—	—
850	$9{\cdot}7 \times 10^3$	$4{\cdot}9 \times 10^{-10}$	0·88
800	$3{\cdot}0 \times 10^4$	$1{\cdot}6 \times 10^{-9}$	0·76
750	$1{\cdot}0 \times 10^5$	$1{\cdot}5 \times 10^{-9}$	0·75
700	$3{\cdot}3 \times 10^5$	$8{\cdot}6 \times 10^{-10}$	0·80
650	$1{\cdot}2 \times 10^6$	$1{\cdot}1 \times 10^{-9}$	0·73
1 100	$1{\cdot}1 \times 10^2$	—	—
805	$1{\cdot}9 \times 10^4$	$1{\cdot}8 \times 10^{-9}$	0·76

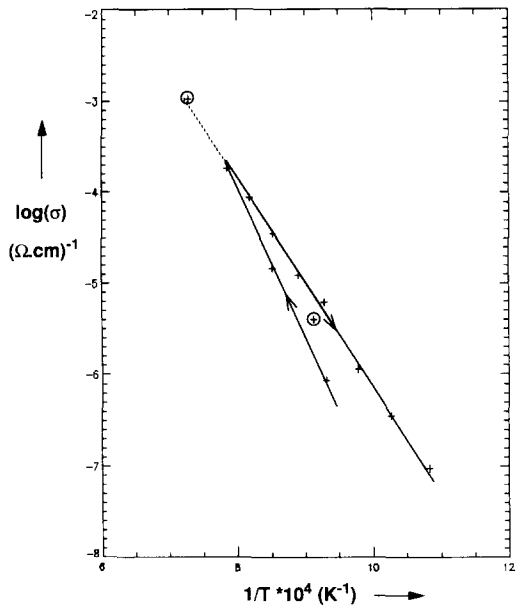

Fig. 4. Arrhenius plot for conductivity of the AlN ceramic showing an activation energy of 2·4 eV.

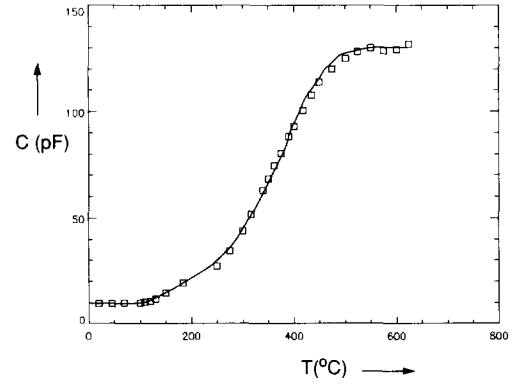

Fig. 5. The measured capacitance of the sample as a function of temperature.

room temperature up to 625°C. Above this temperature reliable measurements of the capacitance becomes impossible due to the measuring frequency of 1 kHz. The measured capacitance as a function of the temperature is shown in Fig. 5. The capacitance of 9 pF measured at room temperature is close to the calculated capacitance from the cell geometry (1×10^{-11} F). The capacitance measured at 600°C is $1{\cdot}3 \times 10^{-10}$ F which is lower than the value calculated from the complex impedance data.

4 Discussion

The high-temperature electrical measurements show an activation energy for conduction of 2·4 eV. From the analysis of the complex impedance spectra it can be concluded that a capacitance has been found which is larger than the expected geometrical capacitance.

The difference between the measured capacitance and the value calculated from the complex impedance data is a result of the fact that the LCR meter is only able to measure ideal capacitances and not constant phase elements. As a result a significant positive deviation from the actual capacitance arises.

The calculated capacitances (Table 1) are much higher than the expected geometrical capacitance of the sample which is estimated at 1×10^{-11} F. This result indicates that the data can be interpreted by using the brick layer model as proposed by Beekmans & Heyne[10] and described by Van Dijk & Burggraaf.[11] In this model for a two-phase ceramic material, conduction along the grain boundaries is negligible, in other words, the resistance of the grain boundaries is much higher than the resistance of the bulk. Applying the brick layer model, the thickness of the grain boundary, d_{gb}, can be estimated by:[11]

$$d_{gb}/D = (C_{geo}/C_{meas}) \cdot (\varepsilon_{gb}/\varepsilon_b)$$

In this formula D is the grain size, C_{geo} is the expected geometrical capacitance, C_{meas} is the measured capacitance (or CPE) and ε_{gb}, ε_b are the dielectric constants for the grain boundary and the bulk phases. For the last term in the equation 11/9 or 16/9 may be used ($\varepsilon(Y_3Al_5O_{12}) = 11$,[12] $\varepsilon(AlN) = 9$,[13] $\varepsilon(YAlO_3) = 16$[14]). The values for $Y_3Al_5O_{12}$ and $YAlO_3$ are used, since these phases were observed as second phases in the sample using X-ray diffraction. The median grain size for the AlN particles has been estimated at about 6 μm. An average value of $1{\cdot}6 \times 10^{-9}$ F is found for the measured capacitance, while a value of 1×10^{-11} F can be calculated for the expected geometrical capacitance. This leads to an estimated range for the thickness of the grain boundary layer of 46–67 nm. For simplicity, average values were taken. However, Wernicke[15] has shown, using computer simulations, that the brick layer model is a reasonable description of ceramic microstructures.

This leads to the conclusion that the AlN grains are covered with a continuous grain boundary phase of which the average thickness is estimated to be between 46 nm and 67 nm. This is supported by the SEM micrographs in Fig. 2. The electrical resistance at high temperatures is fully determined by these grain boundaries. The electrical conductivity of the grain boundary phases is consequently the only information obtained. It is noted that since the phases on the grain boundary are oxides, i.e. $YAlO_3$ and $Y_3Al_5O_{12}$, the conductivity is expected to be independent of the partial nitrogen pressure. This is in agreement with published reports.[1-3] The activation energy for conduction of 2·4 eV which has been observed for this sample has the same order of magnitude as has been reported for $Y_3Al_5O_{12}$ (2·4 eV).[12] The wide range of activation energies for electrical conduction for AlN ceramics, as discussed in the introduction, can be well explained in the

presented model. The use of different sintering dopes, as well as various sintering conditions, will result in a variety of grain boundary phases and different morphologies, which, in fact, dominate the electrical properties of the sintered sample.

It is interesting to discuss the capacitance measurements and especially the temperature dependency of the capacitance. As already discussed, it may be concluded that above 600°C the bulk conductivity of the AlN grains is large compared to the grain boundary conductivity. The temperature dependency of the capacitance shows a decrease below 500°C, which indicates that is this temperature region the grain boundary conductivity and the bulk conductivity are of the same order of magnitude. Below 200°C a value is observed which equals the expected geometrical capacitance. This indicates that below 200°C the resistance of the sample is probably dominated by the bulk resistance of AlN.

In conclusion, it has been shown that in the ceramic sample the AlN grains are almost completely covered with grain boundary phases which the average thickness is estimated to be between 46 nm and 67 nm. Above 600°C these phases, $YAlO_3$ and $Y_3Al_5O_{12}$, completely determine the electrical properties of the sample, which can be interpreted using the brick layer model. With this model the large variety of reported activation energies for electrical conduction and the independence of the conductivity on the partial nitrogen pressure can be explained.

Acknowledgements

Grateful acknowledgements are due to A. G. Mouwen-Tijssen for the X-ray analysis, to C. J. Geenen for the SEM work and to P. V. E. Krusemann for the oxygen and carbon analyses.

References

1. Francis, R. W. & Worrell, W. L., High temperature electrical conductivity of aluminium nitride. *J. Electrochem. Soc.*, **123** (1976) 430–3.
2. Richards, V. L., Tien, T. Y. & Pehlke, R. D., High temperature electrical conductivity of aluminium nitride. *J. Mater. Sci.*, **22** (1987) 3385–90.
3. Yahagi, M. & Goto, K. S., Ionic conductivity of AlN containing Y_2O_3 of Al_2O_3 at 1173–1773 K. *J. Japan Inst. Metals*, **47** (1983) 419–24.
4. Anbreeva, T. U. & Dubovick, T. V., *Diehlektr. Poluprovodn*, **6** (1974) 31–3.
5. Zulfequar, M., Zingh, D. B. & Kumar, A., Effect of various oxide additives on dielectric behaviour of hot pressed AlN ceramic. *Mater. Sci. Techn.*, **5** (1989) 403–5.
6. Slack, G. A., Tanzill, R. A., Pohl, P. O. & Vandersande, J. W., The intrinsic thermal conductivity of AlN. *J. Phys. Chem. Solids*, **48** (1987) 641–7.
7. Harris, J. H., Youngman, R. A. & Teller, R. G., On the nature of the oxygen-related defect in aluminium nitride. *J. Mater. Res.*, **5** (1990) 1763–73.
8. Macdonald, J. R., *Impedance Spectroscopy, Emphasizing Solid Materials and Systems*. John Wiley & Sons, New York, 1987.
9. Boukamp, B. A., Computer program EQUIVALENT CIRCUIT. University of Twente, Enschede, The Netherlands, 1989.
10. Beekmans, N. M. & Heyne, L., Correlation between impedance, microstructure, and composition of calcia-stabilized zirconia. *Electrochim. Acta*, **21** (1976) 303–10.
11. van Dijk, T. & Burggraaf, A. J., Grain boundary effects on ionic conductivity in ceramic $Gd_xZr_{1-x}O_{2-(x/2)}$ solid solutions. *Phys. Stat. Sol. (a)*, **63** (1981) 229–33.
12. Schuh, L., Metselaar, R. & de With, G., Electrical transport and defect properties of Ca- and Mg-doped yttrium aluminium garnet ceramics. *J. Appl. Phys.*, **66** (1989) 2627–32.
13. Collins, A. T., Lightowlers, E. C. & Dead, P. J., Lattice vibration spectra of aluminium nitride. *Phys. Rev.*, **158** (1967) 833–8.
14. Asano, H., Kubo, S., Michikami, O., Satoh, M. & Konada, T., Epitaxial growth of europeum barium copper oxide films on yttrium aluminate single crystals. *Jpn J. Appl. Phys.*, **29** (1990) L1452–4.
15. Wernicke, R., *Advances in Ceramics*, Vol. 1, ed. L. M. Levinson. The American Ceramic Society, Inc., Columbus, Ohio, 1982, 272 pp.